Cold Target Recoil Ion Momentum Spectroscopy

R. Dörner[†‡1], V. Mergel[†], L. Spielberger[†], O. Jagutzki[†], M. Unverzagt[†], W. Schmitt[†], J. Ullrich[*], R.Moshammer[†*] H. Khemliche[‖], M.Prior[‖], R.E. Olson[◇], L. Zhaoyuan, [□], W. Wu[†], C.L. Cocke[‡] and H. Schmidt-Böcking[†]

[†] *Institut für Kernphysik, Universität Frankfurt D60486 Frankfurt, Germany*
[*] *GSI, D64291 Darmstadt, Germany*
[‖] *Lawrence Berkeley National Laboratory, Berkeley, CA 94720*
[◇] *University of Missouri, Rolla*
[□] *Lanzhou University, PR China*
[‡] *Kansas State University, Manhattan, Kansas 66506*

The experimental technique of Cold Target Recoil Ion Momentum Spectroscopy (COLTRIMS) is described. It allows a three dimensional imaging of momentum space of the recoiling ion for all ionizing atomic reaction with 4π solid angle for momentum measurement. The resolution presently achieved is ± 0.035 a.u.. Depending on the collision system this corresponds to a resolution in projectile energy loss of down to $\Delta E/E = 10^{-9}$ and a scattering angle resolution of down to 10^{-9} rad for fast heavy ion collisions. We discuss the experimental technique and some recent results on dynamics of recoil ion production for electron capture, target ionization and projectile electron loss.

INTRODUCTION

For a detailed understanding of charged particle or photon induced electronic transition processes in atoms, ions or molecules experimental techniques are desirable which provide highly differential cross sections, i.e. approaching the ideal 'complete' experiment. The dynamics of reactions such as single or multiple target ionization, projectile ionization, single and multiple electron capture or transfer ionization can be unveiled by fully determining the final state momentum distribution of the reaction products. In this paper we illustrate the new experimental approach of Cold Target Recoil Ion Momentum Spectroscopy (COLTRIMS), which allows a three dimensional imaging of the final state momentum space of the recoiling target ion for any ionizing reaction. This technique combines 4π solid angle detection with a high momentum resolution (<0.1 atomic units (a.u.)). The high detection efficiency

[1]E-mail: Doerner@ikf007.ikf.physik.uni-frankfurt.de

makes COLTRIMS ideally suited for multicoincidence experiments. For example the momentum distribution of other reaction products such as one or more electrons, the emerging projectile (scattering angle) or photons can be easily measured in coincidence to the recoil ion. Thus, it paves the way towards experiments complete in momentum space for all ionizing atomic processes. We briefly describe the experimental technique and then discuss the kinematics of recoil ion production by heavy charged particle impact along with some recent results. We do not discuss the case of photoionization, where COLTRIMS has recently also been successfully applied [1,2].

EXPERIMENTAL TECHNIQUE

The momenta of ions emerging from most atomic reactions is in the range of a few a.u., which is about the width of thermal momentum distribution at room temperature. Therefore the experimental key to enable such measurements is a preparation of an internally cold gas target. First experiments used extended warm or cooled gas cells [3–5] or warm effusive jets [6–9]. The highest resolution was achieved in recent experiments by using precooled supersonic gas jets [10–12].

The He gas is precooled by a cryogenic cold head to 10-30K and than expands through a $30\mu m$ nozzle. Ne and other gases can be used at a higher temperature, to prevent freezing and forming of clusters. The inner part of this supersonic gas jet passes through a skimmer of 0.3mm diameter about 1 cm above the nozzle into the scattering chamber. The internal momentum spread of the target in the direction of the gas jet is determined by the parameters of the expansion and is typically below 0.1 a.u.. The supersonic expansion gives the He atoms an offset velocity of about $v_{jet} = 2$ a.u. at a nozzle temperature of 30 K. In both directions perpendicular to the direction of the jet the momentum spread is typically 0.03 to 0.07 a.u.; this is determined by v_{jet} and the skimmer diameter and its distance to the nozzle.

The gas jet is intersected with the ion, electron or photon beam about 2 cm above the skimmer. Recoil ions created at the intersection region are accelerated by a weak homogeneous electric field (0.3-20 V/cm, depending on the range of momenta expected in the experiment). After passing a field-free drift region they are detected by a two-dimensional position-sensitive channel-plate detector with wedge-and-strip readout. From the time of flight of the ion, measured by a coincidence with the projectile, an electron, photon or a pulsed beam, the charge state is determined and the momentum in field direction is calculated. From the position information on the channel-plate detector and the time-of-flight one obtains the two momentum components perpendicular to the field. One example of this type of spectrometer is shown in figure 1.

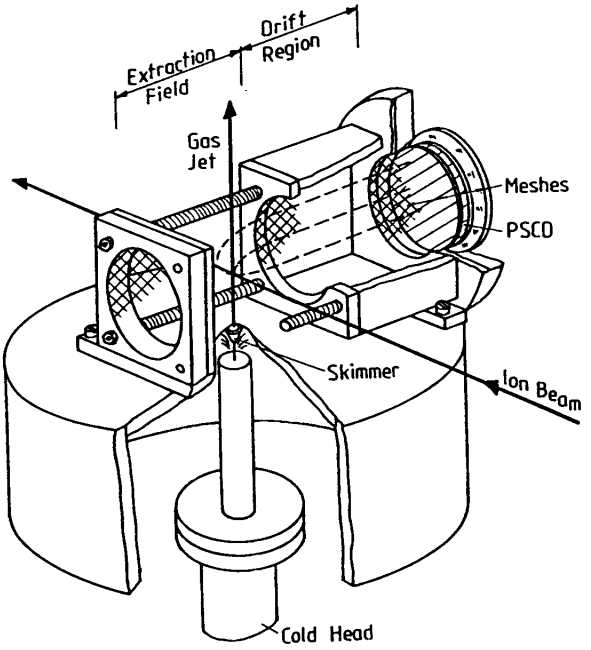

FIG. 1. Example of a gas jet and a spectrometer for COLTRIMS (from ref. 9). The gas nozzle is mounted on a cryogenic cold head. The ions created at the interaction point of gas jet and ion beam are projected by a 0.3V/cm homogeneous electrical field onto a position-sensitive channel-plate detector. The ion time of flight is measured by a coincidence with the projectile or any other reaction product.

In the field direction the momentum measurement becomes insensitive to the different starting points of the ions within the jet due to the time focussing properties of the configuration of the field and drift regions. In the two directions perpendicular to the field the uncertainty of the starting point of the ion limits the momentum resolution of the spectrometer. To circumvent this problem an additional electrostatic lens can be implemented in the field region of the spectrometer which focuses the ions starting from different positions within the jet to the same position on the channel plate.

KINEMATICS OF RECOIL ION PRODUCTION FOR FAST HEAVY PARTICLE IMPACT

For heavy ion collisions the energy loss or gain of the projectile is typically small compared to the total energy of the projectile. Also the scattering angles are in the range of only a few mrad. In this case the momentum components of the recoil ion longitudinal to the beam ($p_{\parallel_{rec}}$) and perpendicular to the beam ($p_{\perp_{rec}}$) are fully decoupled and carry different information about the collision process.

$p_{\perp_{rec}}$ results from the internuclear repulsion (which makes it sensitive to the impact parameter of the collision) and the transverse momentum of the emitted electrons. Thus in a pure capture collision, where no electron is emitted to the continuum, $p_{\perp_{rec}}$ is exactly equal to the transverse projectile momentum given by the projectile scattering angle. For reactions where one or more electrons are emitted to the continuum the transverse momentum of these electrons couples partly to the recoil ion and partly to the projectile transverse motion. The details of this transverse momentum exchange depend strongly on the collision system. For fast collisions the contribution of the electron to $p_{\perp_{rec}}$ is typically in the range of the Compton profile of the initial state of the emitted electron. Thus larger $p_{\perp_{rec}}$ can be related to the impact parameter. [3,13,4,14,5,8,15,9–11,16]. For fast ion collisions a measurement of projectile transverse momentum becomes very inaccurate due to the large initial longitudinal projectile momentum. However $p_{\perp_{rec}}$ can be measured even for these cases with high accuracy. A resolution of ± 0.1 a.u. in the recoil ion transverse momentum, which is typically achieved, corresponds for example in a 1 GeV/u U on He collision to a projectile scattering angle resolution of 10^{-9} rad.

The longitudinal momentum of the recoil ion for a complex reaction involving multiple target ionization, projectile ionization (loss), electron capture and excitation, can be calculated from energy and momentum conservation to be: [17]

$$p_{\parallel_{rec}} = p_{\parallel_{rec}}^{capture} + p_{\parallel_{rec}}^{ionisation} + p_{\parallel_{rec}}^{loss} + p_{\parallel_{rec}}^{excitation} \tag{1}$$

$$p_{\parallel_{rec}}^{capture} = -\frac{n_c v_{pro}}{2} + \frac{Q_c}{v_{pro}}$$

$$p_{\parallel_{rec}}^{ionisation} = \sum_{k=1}^{n_i} \frac{E_{bind}^k + E_{cont}^k}{v_{pro}} - p_{\parallel}^{e_k}$$

$$p_{\parallel_{rec}}^{loss} = \sum_{j=1}^{n_l} \frac{E_{bind}^j + E_{cont}^j}{v_{pro}}$$

$$p_{\parallel_{rec}}^{excitation} = \frac{E_{exc}}{v_{pro}}$$

Atomic units are used throughout this paper. n_c, n_i and n_l is the number of captured, ejected target and projectile electrons. Q_c is the differences in binding energy in the initial and final state summed over all captured electrons (exothermic reactions leading to $Q_c > 0$), E_{bind} and E_{cont} are the binding and continuum energies of the target and projectile electron in their parent rest frame and $p_{\parallel}^{e_k}$ is the longitudinal momentum of target electron k in the final state. E_{exc} is the sum of the excitation energies of target and projectile (if not already counted in Q_c). In the following section we will discuss equation 1 for ionization, electron capture and electron loss along with some examples.

EXPERIMENTAL RESULTS AND DISCUSSION

We first consider the case of a bare projectile, where no projectile electron loss or projectile excitation is possible ($p^{loss}_{\|_{rec}} = 0$). For simplicity we consider one electron processes only. In this case the recoil ion longitudinal distribution has two distinct parts:

$$p_{\|_{rec}} < p^{cusp}_{\|_{rec}} \tag{2}$$

$$p_{\|_{rec}} \geq p^{cusp}_{\|_{rec}} \tag{3}$$

The momentum $p^{cusp}_{\|_{rec}} = E^0_{bind}/v_{pro} - v_{pro}/2$ results from an electron being captured to an continuum state of the projectile [18]. E^0_{bind} is the initial state binding energy of the active electron. Part (2) results from electron capture reactions only, it shows discrete lines related to the quantized Q-value for capture to the different projectile final states. Part (3) emerges from electron emission to the continuum and shows in general no discrete structure.

Figure 2 shows the $p_{\|_{rec}}$ distribution of He^+ ions created by 15 keV p impact. For this collision system all reaction channels are endothermic. The capture to the projectile ground state, which requires the smallest energy transfer, is by far the dominant channel. The capture to the continuum is located at $p^{cusp}_{\|_{rec}}$ =0.77 a.u.. The ionization part of the spectrum which is shown as a solid line in the inset has been measured separately by detecting all emitted electrons in coincidence with the recoil ion. The peak at 2.06 a.u. results from a two electron process where one electron is captured to H(n=1) and simultaneously the target is excited to $He^+(n = 2)$. The resolution of ±0.035 a.u. achieved in this experiment is limited by the internal momentum distribution of the gas jet. An electrostatic lens has been used to compensate for the different starting points of the ions within the 1 mm jet diameter. The resolution correspond to ± 0.7 eV of energy loss of the projectile. As can be seen from eq. 1 this resolution in energy gain depends, only in second order, on the energy spread of the incoming beam. Thus high resolution energy gain spectroscopy becomes possible even for fast heavy ion beams [17,7,11,12]. The recoil ion momentum resolution of ±0.035 a.u. for example corresponds to $\Delta E/E = \pm 0.7 \times 10^{-9}$ for 1GeV/u U on He collisions.

The momentum distribution for ions resulting from ionization strongly depends on the collision system. For low velocities the ions are emitted forward (see inset in figure 2). The main contribution of this forward shift is the term E_{bind}/v_{pro} which reflects the decrease of longitudinal momentum of the projectile which supplies energy to the electron necessary to escape into the continuum. For fast collisions and small perturbation position and shape of the recoil ion longitudinal momentum distribution changes significantly. For 0.5 MeV p on He it is centered close to zero with a width approximately given by the initial state Compton profile [16,19] (see fig. 3).

For these fast collisions the E^k_{bind}/v_{pro} becomes small compared to the typical continuum momenta of the electron. In this perturbative regime the elec-

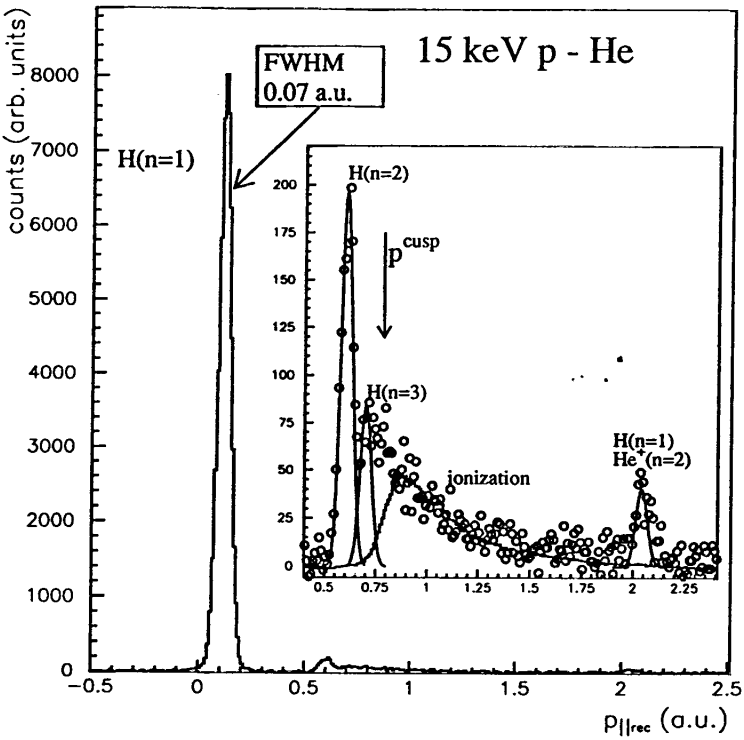

FIG. 2. Longitudinal momentum distribution of He^+ ions from 15 keV proton impact. The dominant peak is due to capture to the projectile ground state. The arrow indicates the position of the capture to the projectile continuum. The full line right of the arrow shows the momentum distribution for ionization only, which has been measured separately by detecting an electron in coincidence with the recoil ion. The momentum resolution is $\pm 0.035 a.u.$, equivalent to an energy gain of $\pm 0.7 eV$ and an recoil ion energy of $\pm 4.5 \mu eV$.

tron is ejected by a short interaction with the projectile leaving the recoil ion with its initial state momentum distribution behind. For fast highly charged ion impact, the recoil-ion emission pattern changes again. In this case the long range force of the highly charged projectile pushes the recoil-ions backward [12,18].

Let us now consider reactions where the projectile is ionized. Projectile ionization can be either a product of an interaction of the target nucleus with the projectile electron (ne), or of one of the target electrons with the projectile electron (ee) [20–23]. In both cases the projectile experiences a backward momentum transfer of at least E^j_{bind}/v_{pro} due to the energy required to overcome the projectile binding energy E^j_{bind}. This momentum is compensated by the active agent in the collision, the target electron (ee) or the target recoil nucleus (ne). In the second case this leads to forward emission of the recoil ion.

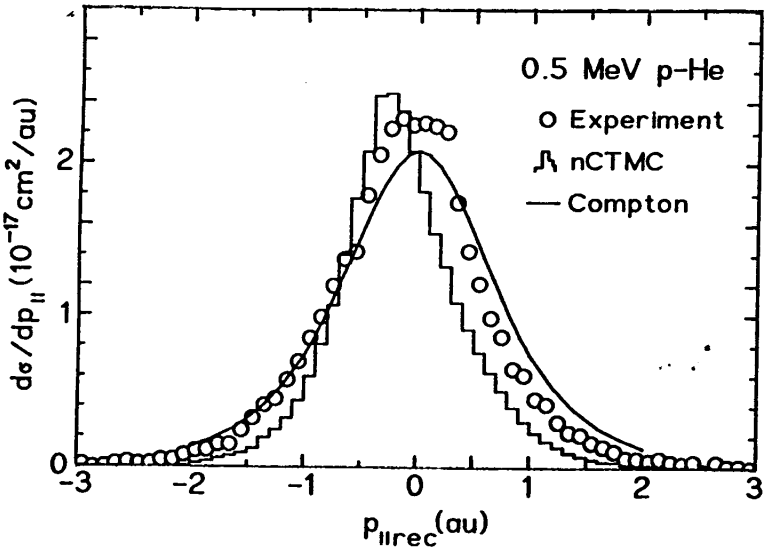

FIG. 3. Longitudinal momentum distribution of He^+ ions from the reaction 0.5 MeV $p + He \rightarrow p + He^+ + e^-$ (from ref. 16). The full line shows the Compton profile of the He atom, the histogram the result of a Classical Trajectory Monte Carlo calculation with two electrons (nCTMC).

For the case of an (ee) interaction the recoil nucleus is only a spectator to the process and gets only a little momentum. $((E^k_{cont})/v_{pro} - p^{ek}_{\|} \approx -E^j_{bind}/v_{pro}$, notation as in eq. 1) Thus, detecting the recoil-ion momentum has allowed, for the first time, experimental separation of the (ne) and (ee) process [10,9,15].

Figure 4 shows the momentum distribution of He^+ ions from simultaneous target and projectile ionization for 1MeV He^+ on He collisions (from ref [10]). The maximum close to zero momentum results from the (ee) interaction. The contribution from the (ne) interaction is shifted forward and to larger transverse momentum transfer, indicating that the cross section for this process peaks at smaller impact parameters than the (ee) contribution [24].

CONCLUSION

We have demonstrated how processes like target ionization, electron capture and projectile electron loss are characterized by very different momentum transfer to the recoil ion. The new experimental technique of COLTRIMS allows to measure this quantity with a unique combination of high resolution

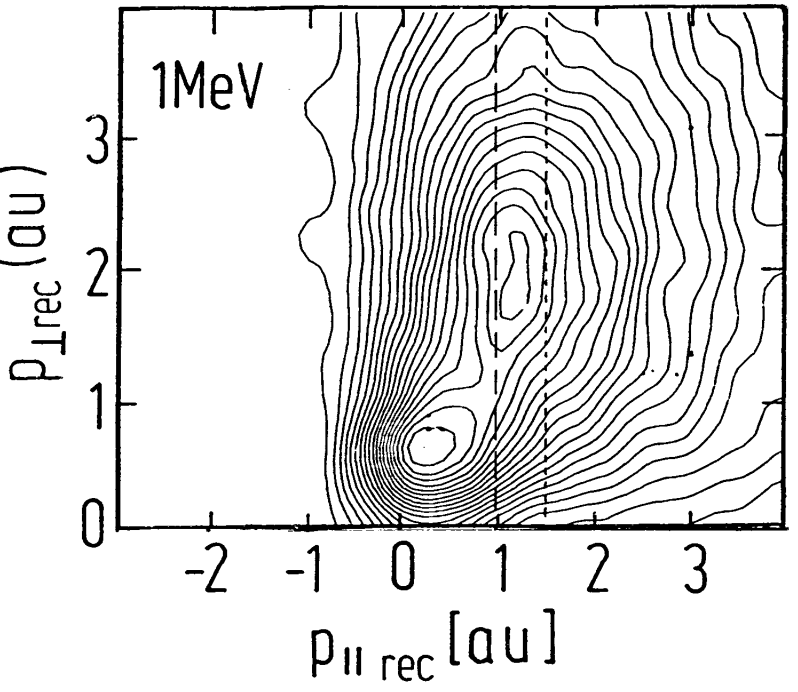

FIG. 4. Longitudinal (to the ion beam) and transverse momentum distribution of He^+ recoil ions from simultaneous target and projectile ionization. The peak close to zero at 1 MeV is due to the (ee) interaction, the second peak is due to the (ne) interaction (from ref (8)).

in momentum space and 4π solid angle. It can easily be combined with detection devices for other reaction products allowing for complete experiments in momentum space for ion, electron, or photon atom and molecule collisions. Since the primary ion beam is not affected by the recoil ion detection, this technique is ideally suited for implementation in storage rings.

I. ACKNOWLEGMENT

The work was financially supported by DFG, BMFT and DOE grant 82ER53128 (KSU) and DOE contract No. DE-AC03-76SF00098 (LBNL). One of us (R.D.) was supported was supported by the Feodor Lynen Progam of the Alexander von Humboldt Stiftung. We also acknowledge financial support from Max Planck Forschungspreis of the Humboldt foundation. We are

thankful to our colleagues W.E. Meyerhof, E. Montenegro, Y.D. Wang, V.D. Rodriguez, C.D. Lin, and U. Buck for helpful discussions.

REFERENCES

1. L. Spielberger, O. Jagutzki, R. Dörner, J. Ullrich, U. Meyer, V. Mergel, M. Unverzagt, M. Damrau, T. Vogt, I. Ali, Kh. Khayyat, D. Bahr, H.G. Schmidt, R. Frahm, and H. Schmidt-Böcking. *Phys. Rev. Lett.*, 74:4615, 1995.
2. T. Vogt. *Diploma Thesis, University Frankfurt 1995, to be published.*
3. J. Ullrich, R.E. Olson, R. Dörner, V. Dangendorf, S. Kelbch, H. Berg, and H. Schmidt-Böcking. *J. Phys*, B22:627, 1989.
4. R. Dörner, J. Ullrich, H. Schmidt-Böcking, and R.E. Olson. *Phys. Rev. Lett*, 63:147, 1989.
5. S. Lencinas, J. Ullrich, R. Dörner, R.E. Olson, W. Wolff, L. Spielberger, S. Hagmann, M. Horbatsch, C.L. Cocke, and H. Schmidt-Böcking. *J. Phys*, B27:287, 1994.
6. V. Frohne, S. Cheng, R. Ali, M. Raphaelian, C.L. Cocke, and R.E. Olson. *Phys. Rev. Lett*, 71:696, 1993.
7. R. Ali, V. Frohne, C.L. Cocke, M. Stöckli, S. Cheng, and M.L.A. Raphaelian. *Phys. Rev. Lett*, 69:2491, 1992.
8. W. Wu, J.P. Giese, Z. Chen, R. Ali, C.L. Cocke, P. Richard, and M. Stöckli. *Phys. Rev.*, A50:502, 1994.
9. W. Wu, R. Ali, C.L. Cocke, V. Frohne, J.P. Giese, B. Walch, K.L. Wong, R. Dörner, V. Mergel, H. Schmidt-Böcking, and W.E. Meyerhof. *Phys. Rev. Lett*, 72:3170, 1994.
10. R. Dörner, V. Mergel, R. Ali, U. Buck, C.L. Cocke, K. Froschauer, O. Jagutzki, S. Lencinas, W.E. Meyerhof, S. Nüttgens, R.E. Olson, H. Schmidt-Böcking, L. Spielberger, K. Tökesi, J. Ullrich, M. Unverzagt, and W. Wu. *Phys. Rev. Lett*, 72:3166, 1994.
11. V. Mergel, R. Dörner, J. Ullrich, O. Jagutzki, S. Lencinas, S. Nüttgens, L. Spielberger, M. Unverzagt, C.L. Cocke, R.E. Olson, M. Schulz, U. Buck, E. Zanger, W. Theisinger, M. Isser, S. Geis, and H. Schmidt-Böcking. *Phys. Rev. Lett*, 74:2200, 1995.
12. R. Moshammer, J. Ullrich, M. Unverzagt, V. Schmidt, P. Jardin, R.E. Olson, R. Mann, R. Dörner, V. Mergel, U. Buck, and H. Schmidt-Böcking. *Phys. Rev. Lett*, 73:3371, 1994.
13. R.E. Olson, J. Ullrich, and H. Schmidt-Böcking. *Phys. Rev.*, A39:5572, 1989.
14. A. Gensmantel, J. Ullrich, R. Dörner, R.E. Olson, K. Ullmann, E. Forberich, S. Lencinas, and H. Schmidt-Böcking. *Phys. Rev.*, A45:4572, 1992.
15. W. Wu, K.L. Wong, E.C. Montenegro, R. Ali, C.Y Chen, C.L Cocke, R. Dörner, V. Frohne, J.P Giese, V. Mergel, W.E. Meyerhof, M. Raphaelian, H. Schmidt-Böcking, and B. Walch. *Phys. Rev.*, A, 1995. submitted.
16. R. Dörner, V. Mergel, L. Zhaoyuan, J. Ullrich, L. Spielberger, R.E. Olson, and H. Schmidt-Böcking. *J. Phys*, B28:435, 1995.
17. R. Dörner, J. Ullrich, O. Jagutzki, S. Lencinas, A. Gensmantel, and H. Schmidt-Böcking. In W.R. MacGillivray, I.E. McCarthy, and M.C. Standage, editors, *Electronic and Atomic Collisions, Invited Papers of the ICPEAC XVII*, page 351. Adam Hilger, 1991.

18. Y.D. Wang, V.D. Rodriguez, and C.D. Lin. *Phys. Rev.*, page accepted for publication, 1995.
19. V.D. Rodriguez, Y.D. Wang, and C.D. Lin. *J. Phys*, accepted for publication as Letter.
20. D.R. Bates and G. Griffin. *Proc. Phys. Soc. London*, A67:663, 1954.
21. D.R. Bates and G. Griffin. *Proc. Phys. Soc. London*, A68:90, 1955.
22. E.C. Montenegro, W.S. Melo, W.E. Meyerhof, and A.G. dePinho. *Phys. Rev. Lett*, 69:3033, 1992.
23. H.-P. Hülskötter, B. Feinberg, W.E. Meyerhof, A. Belkacem, J.R. Alonso, L. Blumenfeld, E.A. Dillard, H. Gould, G.F. Krebs, M.A. McMahan, M.E. Rhoades-Brown, B.S. Rude, J. Schweppe, D.W. Spooner, K. Street, P. Thieberger, and H.E. Wegner. *Phys. Rev.*, 44:1712, 1991.
24. E.C. Montenegro and W.E. Meyerhof. *Phys. Rev.*, A46:5506, 1992.